Journal of
Manufacturing and Materials Processing

MDPI

Article

Thermal Post-Processing of 3D Printed Polypropylene Parts for Vacuum Systems

Pierce J. Mayville [1], Aliaksei L. Petsiuk [2] and Joshua M. Pearce [1,2,3,*]

[1] Department of Materials Science and Engineering, Michigan Technological University, Houghton, MI 49931, USA
[2] Department of Electrical and Computer Engineering, Western University, London, ON N6A 5B9, Canada
[3] Ivey Business School, Western University, London, ON N6A 5B9, Canada
* Correspondence: joshua.pearce@uwo.ca

Abstract: Access to vacuum systems is limited because of economic costs. A rapidly growing approach to reduce the costs of scientific equipment is to combine open-source hardware methods with digital distributed manufacturing with 3D printers. Although high-end 3D printers can manufacture vacuum components, again, the cost of access to tooling is economically prohibitive. Low-cost material extrusion 3D printing with plastic overcomes the cost issue, but two problems arise when attempting to use plastic in or as part of vacuum systems: the outgassing of polymers and their sealing. To overcome these challenges, this study explores the potential of using post-processing heat treatments to seal 3D printed polypropylene for use in vacuum environments. The effect of infill overlap and heat treatment with a readily available heat gun on 3D printed PP parts was investigated in detail on ISO-standardized KF vacuum fitting parts and with the use of computer vision-based monitoring of vacuum pump down velocities. The results showed that infill overlap and heat treatment both had a large impact on the vacuum pressures obtainable with 3D printed parts. Heat treatment combined with 98% infill reliably sealed parts for use in vacuum systems, which makes the use of low-cost desktop 3D printers viable for manufacturing vacuum components for open scientific hardware.

Keywords: 3D printing; additive manufacturing; vacuum systems; post-processing; sealing; vacuum; thermal processing

Citation: Mayville, P.J.; Petsiuk, A.L.; Pearce, J.M. Thermal Post-Processing of 3D Printed Polypropylene Parts for Vacuum Systems. *J. Manuf. Mater. Process.* **2022**, *6*, 98. https://doi.org/10.3390/jmmp6050098

Academic Editor: George-Christopher Vosniakos

Received: 8 August 2022
Accepted: 7 September 2022
Published: 8 September 2022

1. Introduction

Access to vacuum systems has been limited because they are expensive scientific research instruments [1]. One now decade-old [2,3] promising method of reducing costs [4,5] and thereby improving access [6] to scientific equipment is to use open-source hardware methods. In this approach, which can be used to outfit entire labs [7], scientists co-develop custom scientific hardware and then share their design files with an open-source license [8]. Then, other scientists can digitally manufacture components or entire scientific experimental apparatuses with tools such as 3D printers [9,10]. This approach proved particularly effective at overcoming supply chain issues during the COVID-19 pandemic [11]. The ability to digitally manufacture plastic parts is widely accessible with fused filament fabrication (FFF), as it is the most widely available form of additive manufacturing [12,13]. A recent review found the average scientific open hardware device would save over 88% compared to retail costs and over 92% if 3D printing was used [14]. Using 3D printed plastic parts for final product production instead of prototyping has become increasingly popular and can even be seen in consumer products [15–17].

Although plastic is a perfectly suitable material for many applications in one atmosphere, two problems arise when attempting to use plastic in or as part of vacuum systems: (1) the outgassing of polymers and (2) their sealing. Vacuum systems have historically

not utilized polymer parts except for use in gaskets. Polymers outgas volatile compounds trapped in them when under vacuum [18–20]. Previously, the commercially available FFF polymer with the least outgassing was found to be polypropylene (PP) [18].

To produce a vacuum chamber using FFF plastic components, however, is a non-trivial application of 3D printing. FFF polymers have been used in vacuum systems as an insulator [21] and to produce vacuum-sealable surfaces [22]. Sealing ABS FFF parts with VacSeal was shown to significantly reduce outgassing [23–25]. VacSeal is a commercially available silicone-based resin designed to seal leaks in high and UHV vacuum systems [26]. The lowest temperature curing protocol recommended by the manufacturer is 240 °C for 100 h, which is not compatible with commonly accessible FFF polymers.

Sealing these parts is crucial for vacuum systems as they need to be able to hold a high enough vacuum for challenging applications that are vacuum-dependent such as semiconductor processing [24]. Sealing problems are encountered when attempting to use FFF polymers as there is porosity between each of the printed layers [25,27–29]. Altering print parameters was shown to be an effective method to reduce this porosity and seal an FFF part for positive pressures [27,30,31]. Eleven hardware store and industrial sealants were tested [25] for positive pressures. VacSeal has been shown to be an effective sealing method for 3DP parts in negative pressures [24] but has poor outgassing properties [18,23]. Stereolithography is capable of producing pore-free and vacuum-compatible parts [29,32–34] but is not capable of printing PP parts. Therefore, there is a need for a method to seal 3D printed PP for use in vacuum systems.

This study explores the potential of using post-processing heat treatments to seal FFF-processed PP for use in vacuum environments. The effect of infill overlap and heat treatment with a heat gun on FFF PP parts was investigated in detail. PP was chosen for its outgassing properties [18], chemical compatibility [35] and accessibility as a commercially available FFF polymer. KF flanges are ISO-standardized vacuum fittings that provide a vacuum seal by compressing a rubber O-ring between two mating surfaces; here, KF parts were tested for vacuum sealing before and after heat treatment. The results are presented and discussed in the context of using low-cost open-source FFF 3D printing to manufacture custom scientific vacuum components.

2. Materials and Methods

In order to test the viability of the 3D printed parts for vacuum applications, sealing tests were performed with a 3D printed KF40 to KF16 adapter. This was to demonstrate the utility of a functional vacuum part. To do this, the experiments used a ½ hp Alcatel rotary vacuum pump and a Convectron vacuum gauge. The adapter test print samples were fabricated, heat treated and then monitored for their performance under vacuum. An open-source computer vision process was used for datalogging information from the analog vacuum gauge. The combination of 3D print process parameters and the heat treatment were compared to each other and non-heat-treated samples.

2.1. Sample Design

The rendering and 3D printed test part are shown in Figure 1. The adapter was designed with a 2.5 mm wall thickness to accommodate for 0.5 mm, and the width of the extruder nozzle [36] of the infill given print walls was 1 mm. All the 3D printed components were designed using OpenSCAD [37], a script-based OS 3D modeling program. The designs are available in the Open Science Framework [38].

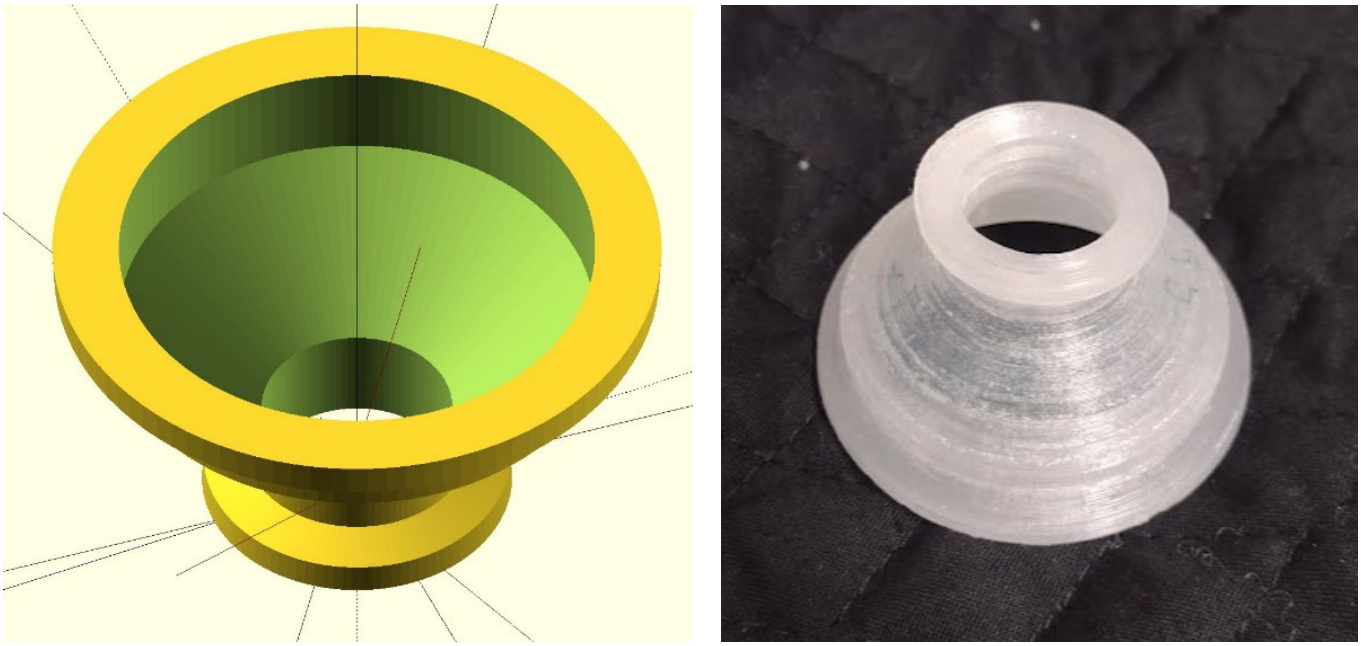

(**a**) (**b**)

Figure 1. (**a**) OpenSCAD rendering and (**b**) photograph of parts designed for sealing tests.

2.2. Fabrication

They were then printed using an open-source RepRap-class [39–41] FFF 3D printer: Lulzbot Taz 6 [42] with an Aerostruder [35,43] and an unpigmented Ultimaker PP filament [44]. The basic print settings used are shown in Table 1.

Table 1. 3D printing process parameters.

Setting	Value	Setting	Value
Layer Thickness	0.18 mm	Flow	102%
Line Width	0.5 mm	Retraction Distance	4.5 mm
Z Seam	Random	Print Speed	50 mm/s
Infill	100%	Minimum Layer Time	12 s

To prevent part warping, a sufficiently large brim was added [45] and was 45 mm for this part. Additionally, bed adhesion was ensured with the application of clear PP packing tape or Ultimaker adhesion sheets [46]. The adhesion sheets have the added benefit of lasting multiple prints without needing replacement. The following methods were tested to seal the PP parts shown in Figure 2: 0, 25, 50 and 98 percent infill overlap settings, printing one part at a time with three replicates and printing three and nine parts at once for a total of 15 replicates. In Figure 2, the outer shell is shown in red and the inner shell is shown in green; yellow paths represent the infill lines in the 3D print.

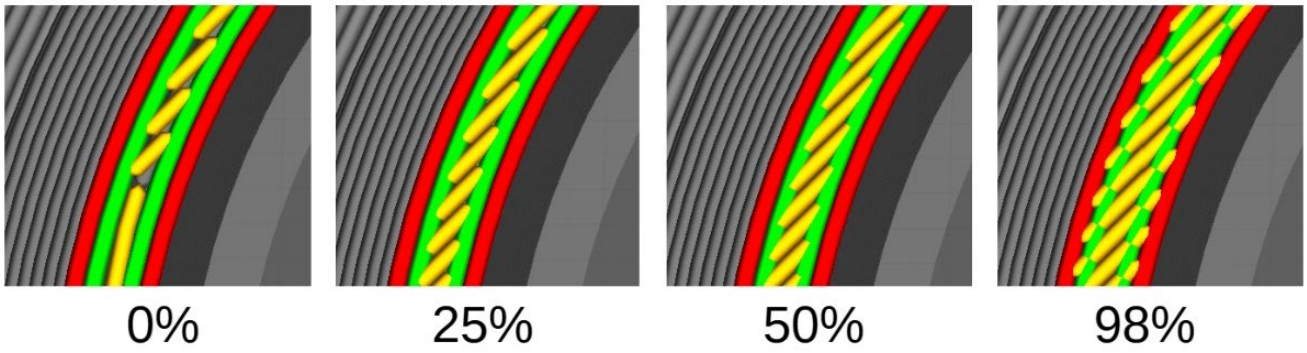

Figure 2. Renderings from Cura Lulzbot showing difference in G-code for overlap percentages. The outer shell is shown in red and the inner shell is shown in green; yellow paths rep-resent the infill lines in the 3D print.

2.3. Heat Treatment

Then, the following heat treatments were applied. Heating parts in an oven was unable to seal the parts without causing deformation. Using a heat gun on its lowest fan speed, where the temperature measured at the gun's nozzle was ~400 °C, allowed parts to be sealed and max out the roughing pump during exploratory experiments. To test this sealing method, the aforementioned heat gun settings were applied to the 3DP parts for ~55 s. This time was chosen as it was the time required to see a visible change in the 3DP part's surface. Heat was applied to the interior of the part and the KF40 surface for ~45 s, with the remaining time spent heating the KF16 surface. This process is shown in a video demonstrating the visible change during sealing heat treatment [38]. Screenshots of this process are shown in Figure 3, and the first and last pictures are before and after sealing, respectively.

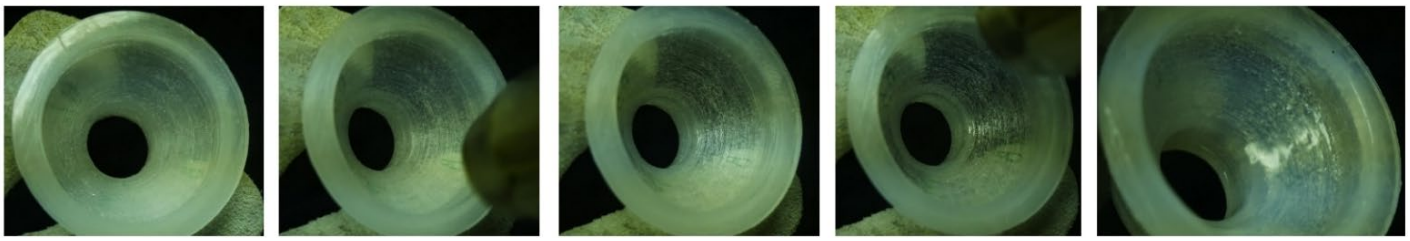

Figure 3. Snapshots from video demonstrating visible change during sealing heat treatment. First and last pictures are before and after sealing, respectively (see Full_Sealing.mp4 video in [38]).

2.4. Vacuum Testing

Each part was tested for vacuum before and after heat treatment with the setup shown in Figure 4. The pressure displayed on the vacuum gauge was recorded with a web camera during pump down. The recording/experiment lasted ten minutes unless either the pressure had stabilized for at least 5 min or the vacuum gauge was bottomed out. The recording was used to generate more accurate pressure readings and pressure versus time plots with an automated computer vision-based gauge reading system [38]. An example of the output from this system is shown in Figure 5.

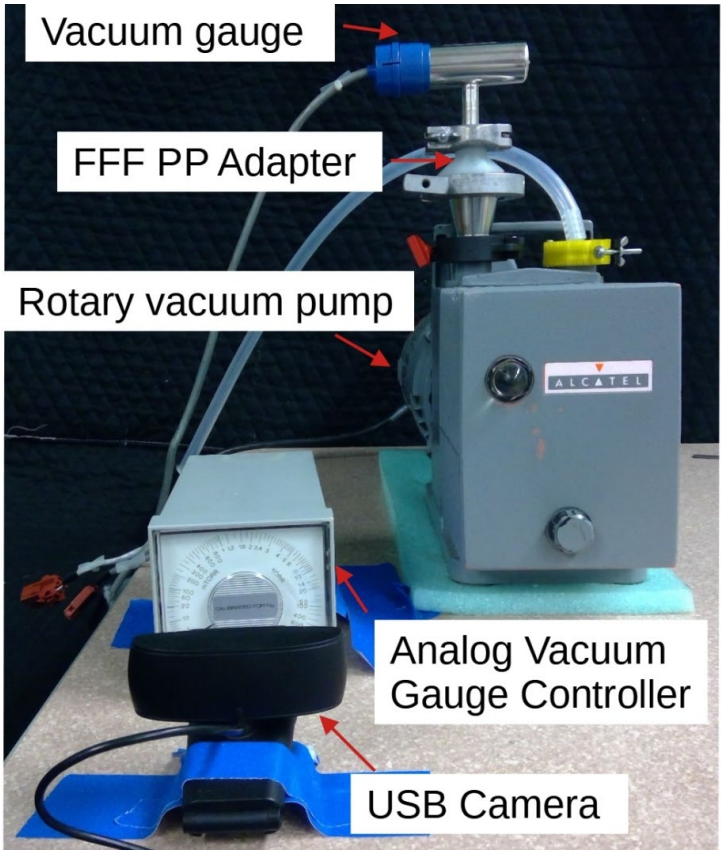

Figure 4. Experimental setup showing pump, FFF part, vacuum gauge, gauge controller and USB camera.

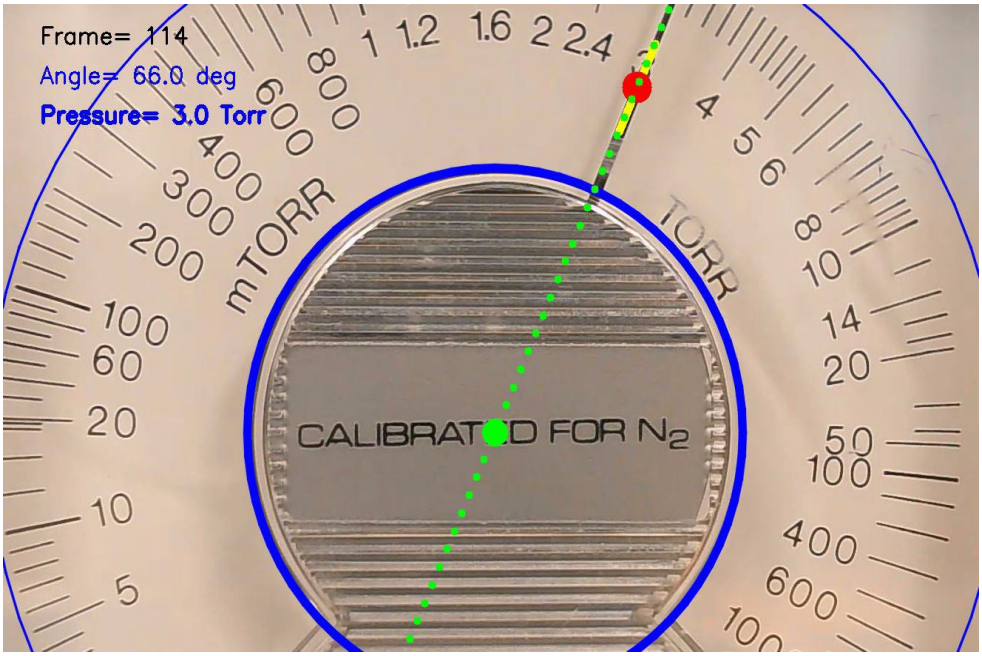

Figure 5. Sample frame from computer vision-based gauge reading system [38] (blue—dial circumference detected with Hough circle transform; yellow—gauge arrow pointer detected with grayscale threshold; red—middle part of the arrow pointer; green—direction to the arrow pointer according to the calculated angle of inclination).

The automated gauge reading system is based on Hough transforms [47–50] and grayscale thresholding. The Hough circle transform was used to detect the visible dial circumference in the image frame and then calculate its center point. To solve this problem, the standard cv2.HoughCircles() function of the OpenCV (Open Source Computer Vision) library was utilized [42]. Appropriate function parameters were selected experimentally. Since the arrow pointer stands out in contrast to the background of the dial, pointer detection was performed based on grayscale segmentation with the empirical threshold values.

The detected coordinates of the center of the dial and the middle part of the pointer allow for calculating the direction and inclination angle of the pointer. Considering the nonlinearity of the sensor scale, conversion of the pointer inclination angle into pressure units was performed on the basis of a preliminary prepared lookup table containing 85 reference values. When processing a video sequence, the inclination angle of the arrow pointer and the pressure corresponding to it are calculated for each frame and recorded in a table file. Knowing the frame rate (frames per second) from the video description, the number of frames is then converted into units of time, which allows for visualizing the pressure dynamics on the timeline (Figures 6 and 7).

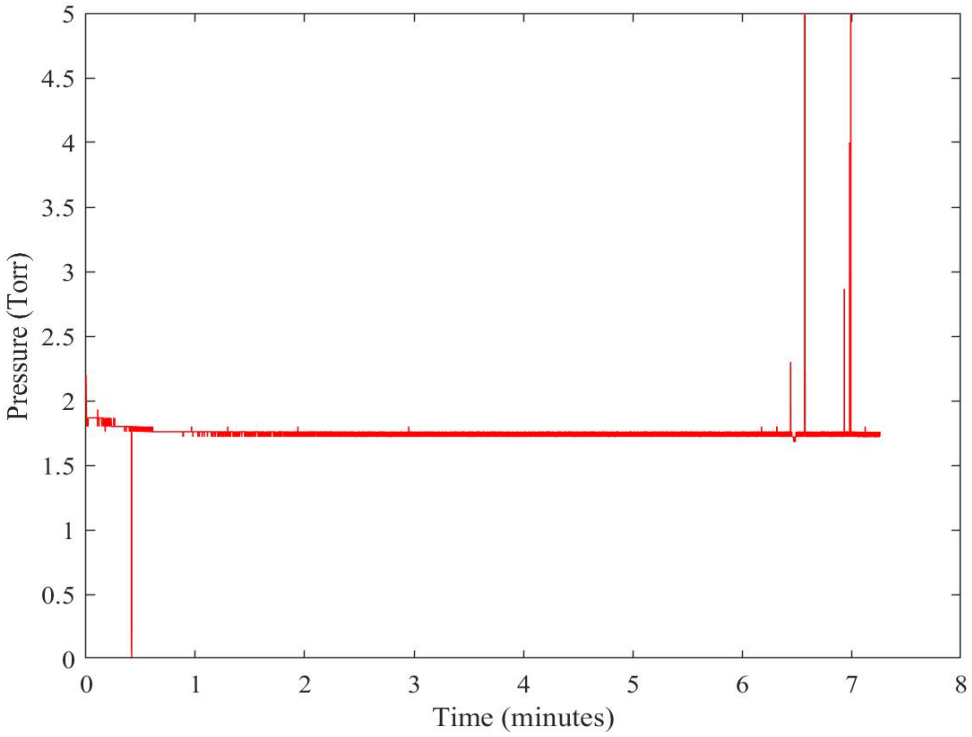

Figure 6. Pressure versus time graph showing last minute with anomalies for 0% overlap parts printed nine at once after heat treatment.

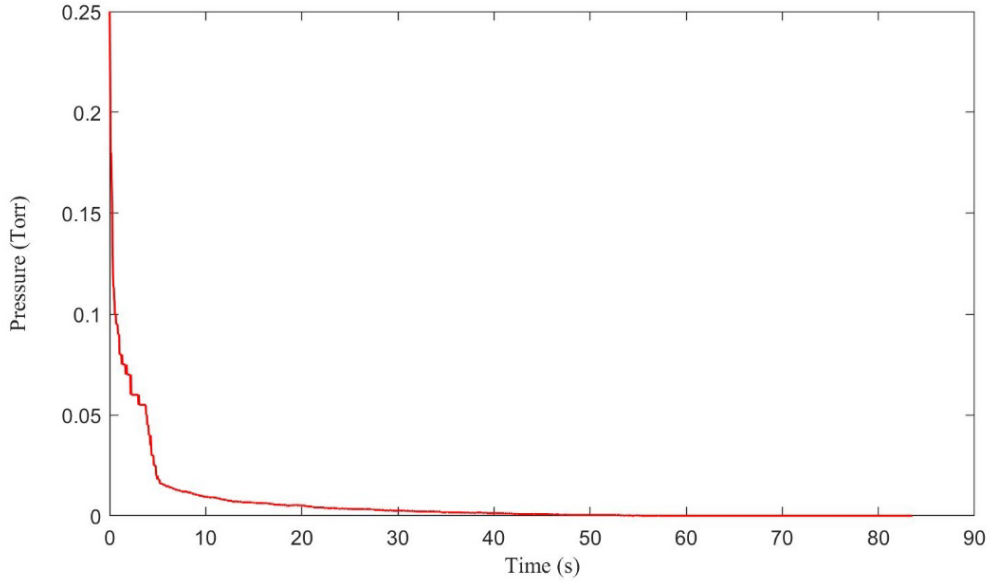

Figure 7. The sealing rate for a fully heat-treated, sealed, 98% overlap part printed nine at once.

The pressure reached by each infill overlap percentage before and after heating was averaged over the last minute in [38]. A 95% confidence interval was used to produce the error bars in the results. The value contributing minute had to be corrected for some of the samples which had anomalies during the last minute of measurement; an example is shown in Figure 6. The value contributing minute was manually selected over a plateau in the data. For fully sealed samples that did not have a full minute of plateau such as that seen in Figure 7, the final pressure was considered to be zero. The final pressure for each set of experimental conditions was recorded and plotted with errors for each 3D printing process parameter variation.

3. Results

As can be seen by the results summarized in Figure 8, the infill overlap had the greatest impact on the relative sealing of the PP parts for vacuum use. This impact was so great, in fact, that graphs a and b for Figure 8 were separated as the impact of heat sealing is not visible for 50 and 98% infill overlap on the scale of 0% overlap. As shown in Figure 8, increasing the overlap percentage reduced the minimum pressure achieved by an untreated part. Increasing the overlap percentage from 0 to 25% and from 25 to 50% reduced the minimum pressure by a factor of 10. Heat treatment, however, also improved the sealing. Heat treatment more than halved the minimum pressure reached by each overlap. The best results were obtained with the highest overlap and heat treatment. Parts printed with 98% infill overlap and sealed after heat treatment had an average, for the 15 repeats, of 0.4 mTorr, with a 95% confidence interval of 0.2 mTorr.

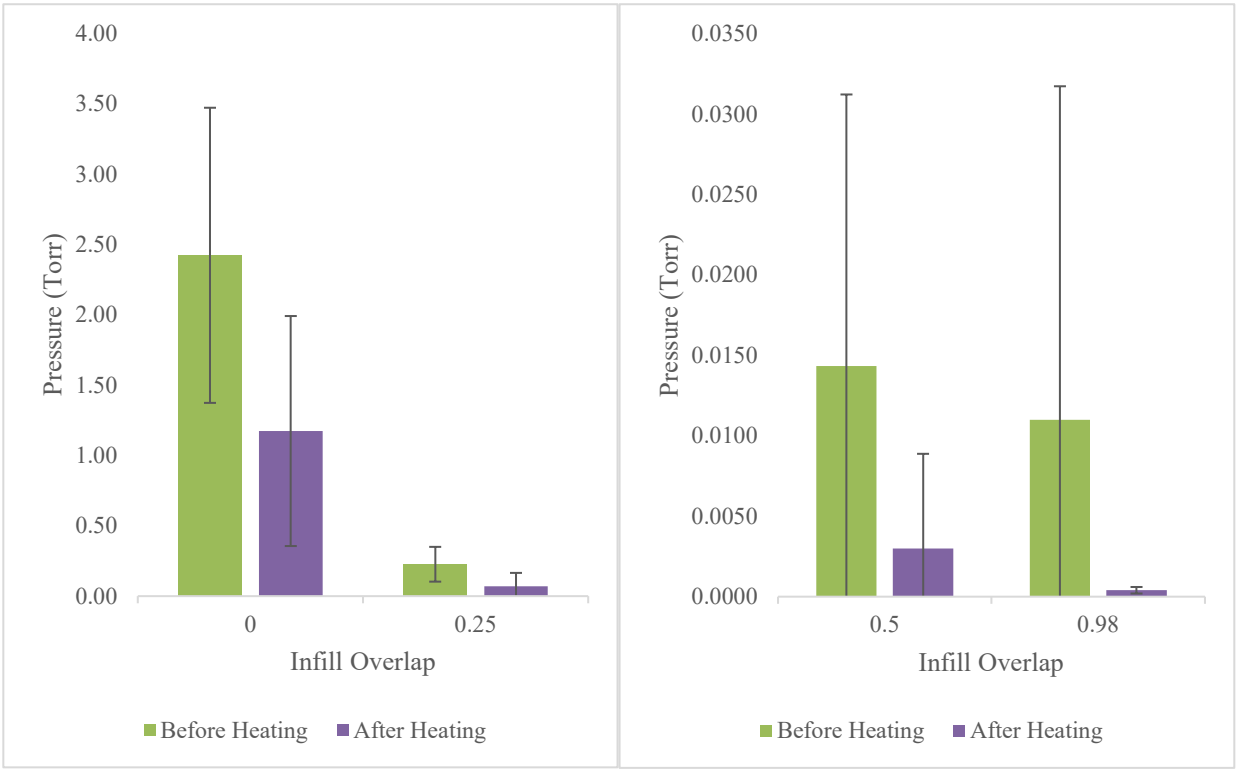

Figure 8. Final pressure reached for each infill overlap percentage before and after heating with 95% confidence intervals. Right graph has excluded 0% and 25% infill overlaps for ease of reading.

4. Discussion

The results of this study show that PP parts can be 3D printed on a low-cost desktop FFF-based printer and have adequate sealing for low-vacuum applications. The thermal post-processing demonstrated in this study can now be added to the other finishing/post-processing methods for 3D printed polymers [51,52]. It has also overcome the high heat limitations of sealing FFF parts with VacSeal [23–26]. The results showed that 3D printed plastic could be used for vacuum components themselves, which goes beyond simply having them in a vacuum environment [53]. Specifically, this process provides substantial opportunities to push this method of manufacturing open hardware for scientific work on vacuum applications [54] for both testing and vacuum processing beyond what has been done before. For example, the ability to utilize custom 3D printed parts in cleanroom environments is also supported [55]. In addition, the process provides an opportunity to radically reduce the costs for vacuum equipment because both higher-cost metal and the necessary machinery could be eliminated. The approach is obviously not adequate for all applications (e.g., those with higher-temperature processing and nothing that approaches the 400 °C used here for post-processing).

This study also has several limitations. While some parts were fully sealed after printing alone, this study found that this is not a reliable way to make a vacuum part. This can be seen in that such parts contributed to the averages for 25% overlap after heating, 50% before and after heating and 98% after heating; the results were not reliable, as can be seen from the confidence interval. This is most likely due to the not fully sealed parts introducing higher values and thus error into the data. The results were all improved with heat treatment, despite the errors observed, and thus, the method investigated here provides a way to increase the reliability of 3D printed vacuum components. It should be pointed out that the results could be improved for 25% and 50% overlaps with the application of a second heat treatment, which may seal the parts better. For this reason, the heat treatment was kept as consistent as possible. Additional heating could have

decreased the minimum pressure reached by the part. The results for 98% overlap (and any other set of prints) before could be improved by replacing the nine parts printed at once with multiples of three at once or one at a time. All the 98% overlap parts printed three at once and one at a time were fully sealed before heating. The average pressure for 98% overlap parts printed one at a time with three replicates at once and with three replicates for six replicates was 0 mTorr, whereas the average for nine printed at once was 18 mTorr. Clearly, printing multiple parts on the same plate created less continuous layers and allowed for more porosity. It can thus be recommended that for vacuum sealed parts, 98% overlap should be used with heat treatment as shown here for a highly reliable sealed part compatible with vacuums with a very low error in the measurements. Further testing would be needed to investigate the role of heat treatment duration and printing multiple parts at once. In addition, the focused thermal processing shown in this study could be compared to the results of whole part annealing [56]. Specifically, an oven or furnace operating at high temperatures could be used to seal the polypropylene parts if a method can be determined to prevent the deformation observed in the initial trial experiments of this study (e.g., with mechanical constraints from a material with a high melting point). This may have an impact on the variations that come from the uneven application of the heat gun, but future work is needed to determine whether this would be beneficial or detrimental to the parts' performance, as the heat gun allows for real-time optimization of the treatment for a given area.

Similar to how computer vision is being used to monitor 3D printing to detect errors [56–58] or correct them [59], this user skill with a heat gun could be incorporated into an artificial intelligence system in the future to adapt to the optical changes in the material as the heat treatment is underway. By comparing images of 3D printed layers undergoing heat treatment from a camera with G-code-based reference images of an ideal process generated with a physics-based rendering engine (i.e., Blender) [60], optimal sealing could be achieved, and the same synthetic images could be used to train an artificial intelligence system to automate the process. This would enable spot heat treatment to be incorporated into smart additive manufacturing for both conventional 3D printing and that specific to vacuum components. This process could then be optimized for a specific part (e.g., small component artifacts may need less heat treatment than thick, larger ones) using computational intelligence (CI) in general and particle swarm optimization (PSO) algorithms in particular that have already shown to be useful in 3D printing process parameter optimization [61]. Lastly, other slicing techniques could be investigated (e.g., concentric ring printing for the outer layers, purposely over-extruding or ironing each layer after deposition).

This sealing method could be applied to more complex designs to construct a vacuum system, such as one for atomic layer deposition (ALD) [1,18] or another chemical vapor deposition process. Thus, rather than having a single vacuum component, as demonstrated here, many (if not all) of the core components for a vacuum system could be fabricated with 3D printing and thermal treatment. The results of this study demonstrated that the treated thermal parts could maintain a vacuum, which could then be coated with a process such as ALD. This system could then be coated using itself to produce parts with improved vacuum properties, i.e., lower outgassing [18,23]. Thus, for example, the interior of a 3D printed and thermally sealed vacuum chamber could be coated with a high-vacuum-compatible ALD layer. Then, it could operate as a conventional ALD chamber for a wide range of materials, including those not compatible with the initial plastic materials.

The sealing method tested here has applications outside of vacuum systems at positive pressures. A sealed PP FFF vessel could be integrated into an open-source bioreactor [62] or utilized as chemical labware [10,23]. Although this study focused on PP for its outgassing and chemical properties, other FFF polymers' mechanical properties could be improved by increasing interlayer bond strength with heat treatment [63,64]. Incorporating a small heat gun into an FFF printer's extruder carriage has the potential to produce sealed or stronger FFF parts without post-processing. Further work is needed in this area to optimize the process parameters and slicing for such a tool head.

5. Conclusions

Optimizing infill overlap settings increased the vacuum that a 3D printed PP part was capable of holding. Printing FFF parts with 98% infill was able to significantly reduce the minimum vacuum pressure a part was capable of holding. Utilizing a heat gun set to ~400 °C for ~55 s to seal the FFF surface exposed to vacuum was found to be effective and improve the minimum vacuum pressure achievable. This heat treatment combined with 98% infill reliably sealed the part for use in vacuum systems, which makes the use of low-cost desktop 3D printers viable for manufacturing vacuum components for scientific hardware.

Author Contributions: Conceptualization, J.M.P.; methodology, P.J.M.; software, A.L.P.; validation, P.J.M., A.L.P. and J.M.P.; formal analysis, P.J.M., A.L.P. and J.M.P.; investigation, P.J.M., A.L.P. and J.M.P.; resources, J.M.P.; data curation, P.J.M. and A.L.P.; writing—original draft preparation, P.J.M., A.L.P. and J.M.P.; writing—review and editing, P.J.M., A.L.P. and J.M.P.; visualization, P.J.M. and A.L.P.; supervision, J.M.P.; project administration, J.M.P.; funding acquisition, J.M.P. All authors have read and agreed to the published version of the manuscript.

Funding: This work was supported by the Witte and Thompson Endowments.

Institutional Review Board Statement: Not applicable.

Informed Consent Statement: Not applicable.

Data Availability Statement: Data are available in [38].

Conflicts of Interest: The authors declare no conflict of interest.

References

1. Lubitz, M.; Medina, P.A.; Antic, A.; Rosin, J.T.; Fahlman, B.D. Cost-Effective Systems for Atomic Layer Deposition. *J. Chem. Educ.* **2014**, *91*, 1022–1027. [CrossRef]
2. Pearce, J.M. Cut Costs with Open-Source Hardware. *Nature* **2014**, *505*, 618. [CrossRef]
3. Fisher, D.K.; Gould, P.J. Open-Source Hardware Is a Low-Cost Alternative for Scientific Instrumentation and Research. *Mod. Instrum.* **2012**, *1*, 8–20. [CrossRef]
4. Pearce, J.M. *Open-Source Lab: How to Build Your Own Hardware and Reduce Research Costs*, 1st ed.; Elsevier: Amsterdam, The Netherlands, 2013.
5. Pearce, J.M. Building Research Equipment with Free, Open-Source Hardware. *Science* **2012**, *337*, 1303–1304. [CrossRef] [PubMed]
6. Niezen, G.; Eslambolchilar, P.; Thimbleby, H. Open-Source Hardware for Medical Devices. *BMJ Innov.* **2016**, *2*, 78–83. [CrossRef] [PubMed]
7. Pearce, J.M. Economic Savings for Scientific Free and Open Source Technology: A Review. *HardwareX* **2020**, *8*, e00139. [CrossRef]
8. Oberloier, S.; Pearce, J.M. General Design Procedure for Free and Open-Source Hardware for Scientific Equipment. *Designs* **2018**, *2*, 2. [CrossRef]
9. Sule, S.S.; Petsiuk, A.L.; Pearce, J.M. Open Source Completely 3-D Printable Centrifuge. *Instruments* **2019**, *3*, 30. [CrossRef]
10. Baden, T.; Chagas, A.M.; Gage, G.; Marzullo, T.; Prieto-Godino, L.L.; Euler, T. Open Labware: 3-D Printing Your Own Lab Equipment. *PLOS Biol.* **2015**, *13*, e1002086. [CrossRef]
11. Maia Chagas, A.; Molloy, J.C.; Prieto-Godino, L.L.; Baden, T. Leveraging Open Hardware to Alleviate the Burden of COVID-19 on Global Health Systems. *PLOS Biol.* **2020**, *18*, e3000730. [CrossRef]
12. Singh, S.; Ramakrishna, S.; Singh, R. Material Issues in Additive Manufacturing: A Review. *J. Manuf. Process.* **2017**, *25*, 185–200. [CrossRef]
13. Zander, N.E.; Gillan, M.; Burckhard, Z.; Gardea, F. Recycled Polypropylene Blends as Novel 3D Printing Materials. *Addit. Manuf.* **2019**, *25*, 122–130. [CrossRef]
14. Kerns, J. Efficient Engineering: Will You Be Downloading 3D-Printed Products Directly from Amazon? Streamlined Online Shopping Presents Challenges to Anyone Trying to Start Consumer 3D Printing. *Mach. Des.* **2018**, *90*, 30–33.
15. The Best 3D Printed Consumer Products. Available online: https://3dprintingindustry.com/news/the-best-3d-printed-consumer-products-148352/ (accessed on 24 February 2022).
16. Brooks, G.; Kinsley, K.; Owens, T. 3D Printing as a Consumer Technology Business Model. *Int. J. Manag. Inf. Syst. IJMIS* **2014**, *18*, 271. [CrossRef]
17. Petersen, E.; Pearce, J. Emergence of Home Manufacturing in the Developed World: Return on Investment for Open-Source 3-D Printers. *Technologies* **2017**, *5*, 7. [CrossRef]

18. Bihari, N.; Heikkinen, I.T.S.; Marin, G.; Ekstrum, C.; Mayville, P.J.; Oberloier, S.; Savin, H.; Karppinen, M.; Pearce, J.M. Vacuum Outgassing Characteristics of Unpigmented 3D Printed Polymers Coated with Atomic Layer Deposited Alumina. *J. Vac. Sci. Technol. A* **2020**, *38*, 53204. [CrossRef]
19. Barton, R.S.; Govier, R.P. A Mass Spectrometric Study of the Outgassing of Some Elastomers and Plastics (Outgassing Properties of Various Organic Polymers and Elastomers Used as Insulators and Seals in Vacuum Systems, Using Bakeable Mass Spectrometer). *J. Vac. Sci. Technol.* **1965**, *2*, 113–122. [CrossRef]
20. Rivera, W.F.; Romero-Talamás, C.A. Vacuum Compatibility of 3-D-Printed Parts. *IEEE Trans. Plasma Sci.* **2016**, *44*, 874–876. [CrossRef]
21. Liu, W.; Huo, Y.; Ke, C.; Cheng, J.; Guo, Y. 3D Printed Polymer Vacuum Insulator. *IEEE Trans. Dielectr. Electr. Insul.* **2021**, *28*, 28–32. [CrossRef]
22. Hong, F.; Tendera, L.; Myant, C.; Boyle, D. Vacuum-Formed 3D Printed Electronics: Fabrication of Thin, Rigid and Free-Form Interactive Surfaces. *SN Comput. Sci.* **2022**, *3*, 275. [CrossRef]
23. Heikkinen, I.T.S.; Marin, G.; Bihari, N.; Ekstrum, C.; Mayville, P.J.; Fei, Y.; Hu, Y.H.; Karppinen, M.; Savin, H.; Pearce, J.M. Atomic Layer Deposited Aluminum Oxide Mitigates Outgassing from Fused Filament Fabrication–Based 3-D Printed Components. *Surf. Coat. Technol.* **2020**, *386*, 125459. [CrossRef]
24. Chaneliere, T. *Vacuum Compatibility of ABS Plastics 3D-Printed Objects*; CNRS, Laboratoire Aimé Cotton: Paris, France, 2017; p. 6.
25. Mireles, J.; Adame, A.; Espalin, D.; Medina, F.; Winker, R.; Hoppe, T.; Zinniel, B.; Wicker, R. Analysis of Sealing Methods for FDM-Fabricated Parts. In Proceedings of the 2011 International Solid Freeform Fabrication Symposium, Austin, TX, USA, 8–10 August 2011; p. 12.
26. SPI Supplies. Vacseal Products. Available online: https://www.2spi.com/category/vacseal/ (accessed on 15 July 2022).
27. Gordeev, E.G.; Galushko, A.S.; Ananikov, V.P. Improvement of Quality of 3D Printed Objects by Elimination of Microscopic Structural Defects in Fused Deposition Modeling. *PLoS ONE* **2018**, *13*, e0198370. [CrossRef] [PubMed]
28. Gelhausen, M.G.; Feuerbach, T.; Schubert, A.; Agar, D.W. 3D Printing for Chemical Process Laboratories I: Materials and Connection Principles. *Chem. Eng. Technol.* **2018**, *41*, 618–627. [CrossRef]
29. Johannink, T.; Kreuzer, E.; Solowjow, E. Sealing of Machine Parts and Modules Manufactured with Desktop 3D Printers. *Konstruktion* **2017**, *69*, 63–73. [CrossRef]
30. Lederle, F.; Kaldun, C.; Namyslo, J.C.; Hübner, E.G. 3D-Printing inside the Glovebox: A Versatile Tool for Inert-Gas Chemistry Combined with Spectroscopy. *Helv. Chim. Acta* **2016**, *99*, 255–266. [CrossRef]
31. Kitson, P.J.; Glatzel, S.; Chen, W.; Lin, C.-G.; Song, Y.-F.; Cronin, L. 3D Printing of Versatile Reactionware for Chemical Synthesis. *Nat. Protoc.* **2016**, *11*, 920–936. [CrossRef]
32. AL-Hasni, S.; Santori, G. 3D Printing of Vacuum and Pressure Tight Polymer Vessels for Thermally Driven Chillers and Heat Pumps. *Vacuum* **2020**, *171*, 109017. [CrossRef]
33. Povilus, A.P.; Wurden, C.J.; Vendeiro, Z.; Baquero-Ruiz, M.; Fajans, J. Vacuum Compatibility of 3D-Printed Materials. *J. Vac. Sci. Technol. Vac. Surf. Films* **2014**, *32*, 33001. [CrossRef]
34. Bergin, M.; Myles, T.A.; Radić, A.; Hatchwell, C.J.; Lambrick, S.M.; Ward, D.J.; Eder, S.D.; Fahy, A.; Barr, M.; Dastoor, P.C. Complex Optical Elements for Scanning Helium Microscopy through 3D Printing. *J. Phys. Appl. Phys.* **2021**, *55*, 95305. [CrossRef]
35. Heikkinen, I.T.S.; Kauppinen, C.; Liu, Z.; Asikainen, S.M.; Spoljaric, S.; Seppälä, J.V.; Savin, H.; Pearce, J.M. Chemical Compatibility of Fused Filament Fabrication-Based 3-D Printed Components with Solutions Commonly Used in Semiconductor Wet Processing. *Addit. Manuf.* **2018**, *23*, 99–107. [CrossRef]
36. LulzBot TAZ Aerostruder Tool Head. Available online: https://www.farnell.com/datasheets/2632879.pdf (accessed on 30 June 2022).
37. OpenSCAD. Available online: https://openscad.org (accessed on 24 February 2022).
38. Pearce, J.M.; Mayville, P.; Petsiuk, A. Heat Treating 3DP Tests. 2021. Available online: https://osf.io/36jch/ (accessed on 8 August 2022).
39. Jones, R.; Haufe, P.; Sells, E.; Iravani, P.; Olliver, V.; Palmer, C.; Bowyer, A. RepRap—The Replicating Rapid Prototyper. *Robotica* **2011**, *29*, 177–191. [CrossRef]
40. Sells, E.; Bailard, S.; Smith, Z.; Bowyer, A.; Olliver, V. RepRap: The Replicating Rapid Prototyper: Maximizing Customizability by Breeding the Means of Production. In *Handbook of Research in Mass Customization and Personalization*; World Scientific Publishing Company: Singapore, 2009; Volume 2, pp. 568–580, ISBN 978-981-4280-25-9.
41. Bowyer, A. 3D Printing and Humanity's First Imperfect Replicator. *3D Print. Addit. Manuf.* **2014**, *1*, 4–5. [CrossRef]
42. LulzBot TAZ 6. Available online: https://www.lulzbot.com/store/printers/lulzbot-taz-6 (accessed on 24 February 2022).
43. OHAI: Open Hardware Assembly Instructions. Available online: https://ohai.lulzbot.com/project/lulzbot-taz-6-aerostruder-tool-head-installation/accessories/ (accessed on 30 June 2022).
44. Ultimaker Polypropylene Filament-2.85 mm (0.5 kg). Available online: https://www.matterhackers.com/store/l/ultimaker-polypropylene-filament-300mm/sk/MMFT7T7W (accessed on 24 February 2022).
45. Bachhar, N.; Gudadhe, A.; Kumar, A.; Andrade, P.; Kumaraswamy, G. 3D Printing of Semicrystalline Polypropylene: Towards Eliminating Warpage of Printed Objects. *Bull. Mater. Sci.* **2020**, *43*, 1–5. [CrossRef]
46. Ultimaker 2+/3 Adhesion Sheets-Pack of 25. Available online: https://www.matterhackers.com/store/l/ultimaker-adhesion-sheets/sk/MNS7KT48 (accessed on 24 February 2022).

47. Hough, P.V.C. Machine Analysis of Bubble Chamber Pictures. In Proceedings of the International Conference on High Energy Accelerators and Instrumentation, Geneva, Switzerland, 14–19 September 1959.
48. Hough, P.V.C. Method and Means for Recognizing Complex Patterns. U.S. Patent 3,069,654, 18 December 1962.
49. Duda, R.O.; Hart, P.E. Use of the Hough Transformation to Detect Lines and Curves in Pictures. *Commun. ACM* **1972**, *15*, 11–15. [CrossRef]
50. Open Source Computer Vision (OpenCV): Hough Circle Transform. Available online: https://docs.opencv.org/4.x/da/d53/tutorial_py_houghcircles.html (accessed on 29 July 2022).
51. Dizon, J.R.C.; Gache, C.C.L.; Cascolan, H.M.S.; Cancino, L.T.; Advincula, R.C. Post-Processing of 3D-Printed Polymers. *Technologies* **2021**, *9*, 61. [CrossRef]
52. Karakurt, I.; Lin, L. 3D Printing Technologies: Techniques, Materials, and Post-Processing. *Curr. Opin. Chem. Eng.* **2020**, *28*, 134–143. [CrossRef]
53. Johnson, P.R.; Copeland, P.M.; Ayodele, A.O.; Tarekegn, E.N.; Bromley, S.J.; Harrell, W.R.; Sosolik, C.E.; Marler, J.P. In-Vacuum Performance of a 3D-Printed Ion Deflector. *Vacuum* **2020**, *172*, 109061. [CrossRef]
54. Zwicker, A.P.; Bloom, J.; Albertson, R.; Gershman, S. The Suitability of 3D Printed Plastic Parts for Laboratory Use. *Am. J. Phys.* **2015**, *83*, 281–285. [CrossRef]
55. Pasanen, T.P.; von Gastrow, G.; Heikkinen, I.T.S.; Vähänissi, V.; Savin, H.; Pearce, J.M. Compatibility of 3-D Printed Devices in Cleanroom Environments for Semiconductor Processing. *Mater. Sci. Semicond. Processing* **2019**, *89*, 59–67. [CrossRef]
56. Nuchitprasitchai, S.; Roggemann, M.C.; Pearce, J.M. Three Hundred and Sixty Degree Real-Time Monitoring of 3-D Printing Using Computer Analysis of Two Camera Views. *J. Manuf. Mater. Processing* **2017**, *1*, 2. [CrossRef]
57. Paraskevoudis, K.; Karayannis, P.; Koumoulos, E.P. Real-Time 3D Printing Remote Defect Detection (Stringing) with Computer Vision and Artificial Intelligence. *Processes* **2020**, *8*, 1464. [CrossRef]
58. Petsiuk, A.L.; Pearce, J.M. Open Source Computer Vision-Based Layer-Wise 3D Printing Analysis. *Addit. Manuf.* **2020**, *36*, 101473. [CrossRef]
59. Jin, Z.; Zhang, Z.; Gu, G.X. Autonomous In-Situ Correction of Fused Deposition Modeling Printers Using Computer Vision and Deep Learning. *Manuf. Lett.* **2019**, *22*, 11–15. [CrossRef]
60. Petsiuk, A.; Pearce, J.M. Towards Smart Monitored AM: Open Source in-Situ Layer-Wise 3D Printing Image Anomaly Detection Using Histograms of Oriented Gradients and a Physics-Based Rendering Engine. *Addit. Manuf.* **2022**, *52*, 102690. [CrossRef]
61. Oberloier, S.; Whisman, N.G.; Pearce, J.M. Finding Ideal Parameters for Recycled Material Fused Particle Fabrication-Based 3D Printing Using an Open Source Software Implementation of Particle Swarm Optimization. *3D Print. Addit. Manuf.* **2022**. [CrossRef]
62. Holcomb, G.; Caldona, E.B.; Cheng, X.; Advincula, R.C. On the Optimized 3D Printing and Post-Processing of PETG Materials. *MRS Commun.* **2022**, *12*, 381–387. [CrossRef]
63. Wong, B.G.; Mancuso, C.P.; Kiriakov, S.; Bashor, C.J.; Khalil, A.S. Precise, Automated Control of Conditions for High-Throughput Growth of Yeast and Bacteria with EVOLVER. *Nat. Biotechnol.* **2018**, *36*, 614–623. [CrossRef] [PubMed]
64. Bhandari, S.; Lopez-Anido, R.A.; Gardner, D.J. Enhancing the Interlayer Tensile Strength of 3D Printed Short Carbon Fiber Reinforced PETG and PLA Composites via Annealing. *Addit. Manuf.* **2019**, *30*, 100922. [CrossRef]